Accuracy and Resolution of SWOT Altimetry: Foundation Seamounts

Yao Yu[1], David Sandwell[1], Gerald Dibarboure[2], Curtis Chen[3], Jinbo Wang[3]

1- Scripps Institution of Oceanography, La Jolla, USA
2- Centre National d'Etudes Spatiales, Toulouse, France
3- Jet Propulsion Laboratory, Pasadena, USA

Abstract

We assess the accuracy and spatial resolution of the SWOT swath altimeter for measuring marine gravity anomalies. The analysis is performed at the Foundation seamounts in the South Pacific where we developed a highly accurate gravity field by combining the long-wavelength (> 30 km) gravity field derived from previous nadir altimeters with the shorter wavelength gravity field from the seafloor topography as constrained by the ship gravity. In this region, slope of the ocean variability is 50-100 times smaller than the gravity/slope signal of the seamounts so can be ignored in the analysis. Each SWOT cycle can deliver gravity anomaly/sea surface slope with an accuracy of 2.7 mGal/μrad and a spatial resolution of 14 km, with accuracy diminishing when significant wave height (SWH) exceeds ~3 meters. Averaging repeated SWOT measurements improves the accuracy and resolution. For example, we expect that averaging just 10 repeats (7 months) results in accuracy/resolution that matches the best marine gravity maps based on 230 months of nadir altimetry. With a mission lasting over a year, SWOT promises a substantial leap in marine gravity accuracy and resolution, uncovering previously uncharted details of the seafloor, including thousands of uncharted seamounts.

Introduction

The Foundation seamounts is a 1400-km long chain of approximately 40 large seamounts (2-4 km tall) constructed on young seafloor discovered by a combination of sparse ship soundings and satellite altimeter-derived gravity [Mammericks 1992]. They were named the Foundation seamounts to acknowledge the contribution of the National Science Foundation to the exploration of the Pacific Ocean. Since their discovery using sparse data, there have been two major mapping and sampling cruises to these seamounts. In February-March 1995 the German research vessel *Sonne* undertook a geological study of the Foundation Seamount Chain [Devey et al., 1995]. The aim of the cruise was to map and sample the chain in order to collect geological and geophysical data on its evolution and its interaction with the Pacific-Antarctic Ridge (PAR) spreading axis. In January-February, 1997 a more extensive multibeam and gravity survey was carried out by the *L' Atalante* using a dual multibeam sonar and shipboard gravimeter with a track spacing of 14 km to obtain nearly full bathymetry coverage (Figure 1).

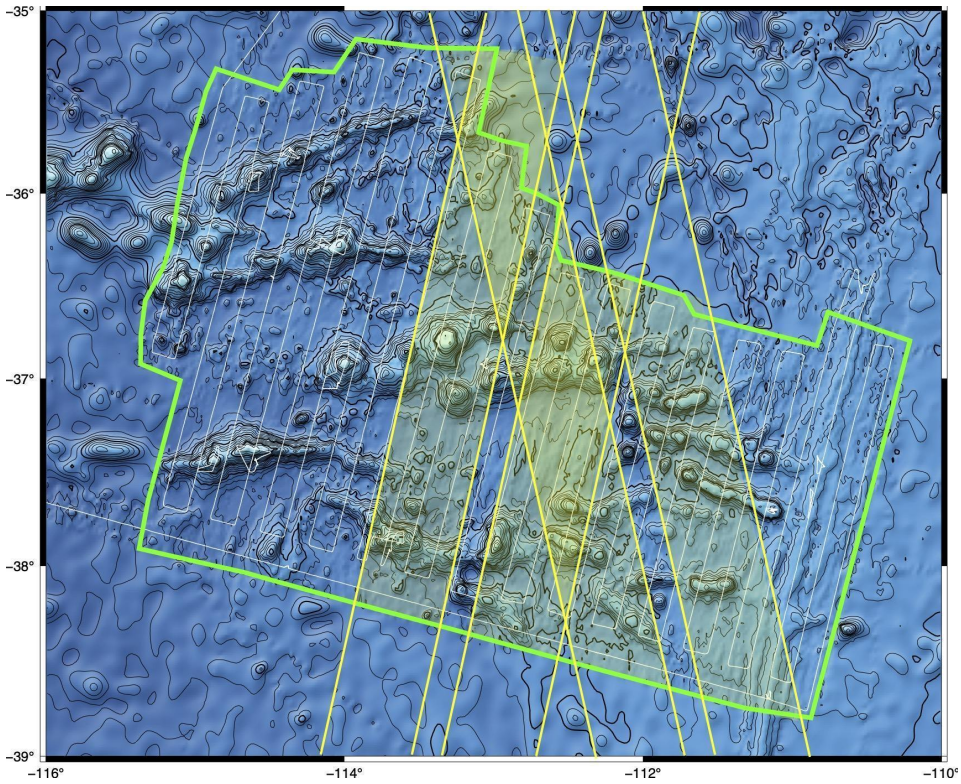

Figure 1. Contours of seafloor topography of the Foundation seamounts. White lines show ship tracks where gravity and multibeam bathymetry was collected. Green line shows perimeter of multibeam coverage. Yellow polygons with shading mark the swaths of the SWOT altimeter.

These seamounts have some unique characteristics that make it an ideal location for validation of SWOT measurements of sea surface height (SSH) and sea surface slope (SSS):

1) The seamounts formed on very young seafloor with age ranging from 0 to 9 Ma so the mean ocean depth varies from 2600 m to 3500 m. This shallow average depth results in a factor of 4.5 times lower attenuation of the short-wavelength gravity field compared to similar seamounts formed on typical ocean lithosphere, where the mean ocean depth is 4500 m. Therefore, the short wavelength (~6 km) gravity signal at the sea surface is relatively large.
2) Because the seafloor is young and far from sources of sediment supply, it is mostly barren rock having a relative uniform density of 2550 to 2750 kg m^{-3} [Maia and Arkani-Hamed, 2002]. In addition, the seamounts are nearly locally compensated by very thin elastic plates (1-4 km). This results in a relatively uniform gravity to topography ratio at wavelengths less than about 60 km.
3) Within the areas of the 1-day SWOT coverage there are approximately 30 closely-spaced volcanic edifices having heights ranging from 1500 to 3500 m. These produce gravity peaks with very large amplitudes (20-120 mGal) and short wavelengths (Figure 2 and Figure S1). The accuracy of the shipboard gravity is better than 1 mGal so the signal to noise ratio exceeds 100.

4) The short wavelength sea surface slope variability (> 18 km) in the region is relatively low (e.g., sea surface slope variability of ~2 microradians (μrad, 1 μrad = 10^{-6} which corresponds to ~1 mGal) [Yu et al., 2023]. The uncertainty in the mean slope is between 0.5 and 2 μrad depending on the number of repeat altimeter profiles. This oceanographic "noise" is 50-100 times smaller than the gravity signal so can be largely ignored in our analysis of SWOT data.

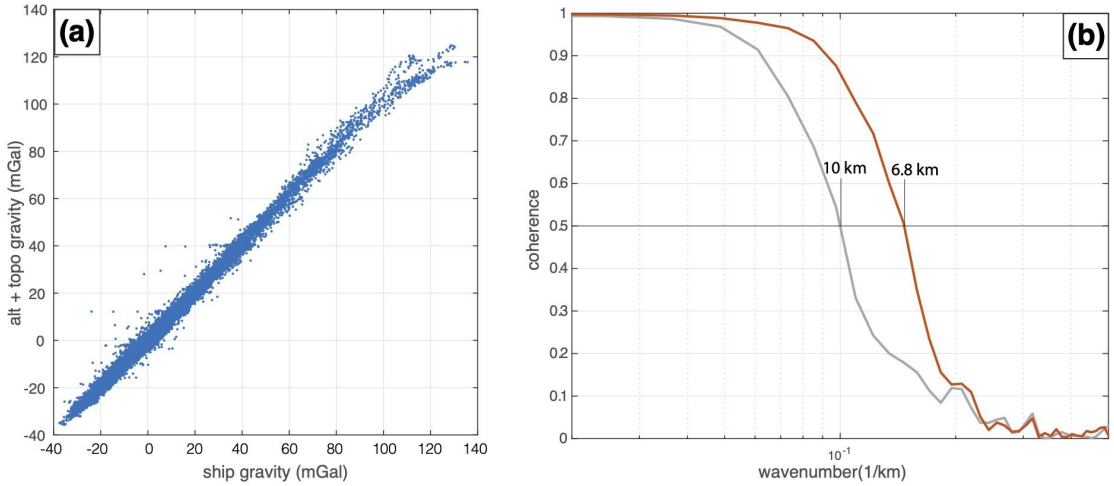

Figure 2. (a) Combined model gravity anomaly versus shipboard gravity (mean difference 0.215 mGal, median absolute deviation 1.42 mGal). (b) (grey) Coherence between altimeter-only gravity and shipboard gravity falls to 0.5 at a wavelength of 10 km. (red) Coherence between combined gravity and ship gravity falls to 0.5 at a wavelength of 6.8 km. There is some coherent signal at 5.5 km wavelength so a sampling of 2.7 km will be the maximum spacing to resolve this wavelength.

The focus of this paper is to assess the accuracy and resolution of SWOT altimetry [Fu et al., 2009; Morrow et al., 2019]. We analyze the Level 2 ocean, low resolution mode L2_LR_SSH beta pre-validated version [Stiles et al., 2023] in the 1-day repeat orbit, in conjunction with the Level 3 low resolution mode products [Dibarboure et al, in prep]. To achieve this objective, we need a grid of mean sea surface (MSS – approximately the geoid) height or SSS that is at least as accurate as the SWOT data. Current MSS and SSS grids are accurate to a few cm and a few μrad, respectively [Schaeffer et al., 2023]. Moreover, the altimeter-based grids cannot resolve wavelengths less than about 16 km because the data are filtered to reduce the noise from ocean waves and other environmental factors. Preliminary results of SWOT sea surface anomaly show residual gravity signals so the current MSS grids are inadequate.
[https://swotst.aviso.altimetry.fr/programs/2023-swot-st-program].

Higher accuracy and resolution MSS/SSS can be achieved at the Foundation seamounts using a combination of multibeam sonar and gravity collected over this area. Yu et al, [2021] proposed a similar analysis for the evaluation of the SWOT data in the South China Sea. The basic approach is to constrain the longer wavelength SSS (> 30 km) with the altimeter-derived products, and the shorter wavelength SSS (<30 km) using the multibeam sonar bathymetry as input to a 3-D isostatically compensated gravity model

which includes sea surface gradient as output. Details of the analysis are presented in the **Supplementary Material**. The important parameter is the crustal density and this is adjusted so the combined gravity model best matches the gravity profile observed by the ship.

Then we will compare the SWOT data collected over the Foundation Seamounts, to the SSS grids (model grid). We first compare the along- and across-track slope grids from SWOT with the corresponding east and north model slopes projected into the along- and cross-track directions. This analysis reveals the slope noise for single passes of SWOT data. In addition, this analysis reveals the magnitude of the SWOT interferometer roll errors. Further analysis shows that the SWOT slope noise depends strongly on the significant wave height (SWH) and distance to the central nadir. We then average, or stack, many repeats of SWOT data to determine how the SSS noise improves as the number in the stack increases. Finally, we perform a cross spectral analysis of the along-track slopes of SWOT to the model slopes and establish the spatial resolution of the SWOT data for a single pass as well as the stack. The results of the analysis provide information on how to best process 2 km resolution SWOT data for use in the recovery of short-wavelength SSS models and gravity anomalies. The analysis also informs the physical oceanographic community on the smallest resolvable ocean dynamic signals versus their wavelength in the presence of environmental noise.

Methods

Our analysis begins with the level-2 beta pre-validated version, low resolution, expert (L2_LR_SSH_Expert) data produced by the SWOT project [Stiles et al., 2023]. Data are provided as passes that extend ½ of an orbit either running from southwest to northeast (ascending) or northwest to southeast (descending). The swath data are stored on a 2 km by 2 km grid with cells oriented in the along-track (a) and cross-track directions (c). We create a corrected sea surface height (SSH) as SSH = ssha_karin + mean_sea_surface_cnescls + height_cor_xover. ssha_karin is the sea surface height anomaly from the KaRIn measurement, with solid earth tide, ocean tide, coherent internal tide, pole tide, and dynamic atmospheric correction applied. mean_sea_surface_cnescls is the CNES_CLS_15 mean sea surface height above the WGS84 reference ellipsoid. This mean sea surface model lacks short-wavelength resolution but is the current embedded reference in the SWOT L2 product. height_cor_xover is the height correction from crossover calibration. These variable names are documented in the L2_LR_SSH_Expert netcdf files as well as the corresponding documentation [Stiles, 2023]. Bad data are optionally eliminated using the *ssha_karin_qual.* The processing also uses the matching grids of *longitude* (e) and *latitude* (n).

In addition to the SWOT data we use global grids of east and north deflection of the vertical based on traditional altimetry [Sandwell et al., 2021]. The latest version V32 of these grids are available at https://topex.ucsd.edu/pub/global_grav_1min/. The accuracy of these vertical deflection grids is improved using the multibeam bathymetry data as described in the **Supplementary Material**. The accuracy of the model east and north grids is ~1.96 microradian based on the comparison with ship gravity (Figure 2a)

and the resolution is 6.8 km based on the cross-spectral coherence between the ship gravity and the gravity from the transformed model slope grids.

Two passes of SWOT data (011 and 026) from the 1-day repeat orbit are windowed in an area of the Foundation seamounts (-116 to -110 longitude, and -39 to -35 latitude). There are ~90 cycles in each pass that enable the analysis of single cycles or averages (stacks) of up to 90 cycles. We are interested in the sea surface slope so we take the gradient of the SSH data for each cycle in both passes. This results in 2-D grids of along-track and cross track slope. We then use the pyGMT command *grdtrack* to sample the model east and north slope grids at the same locations as the windowed SWOT grids. We project the north and east model grids into the directions of the along-track and cross-track slopes as follows:

$$s_e = \frac{\partial h}{\partial e},\ s_n = \frac{\partial h}{\partial n},\ s_c = \frac{\partial h}{\partial c},\ \ s_a = \frac{\partial h}{\partial a}. \tag{1}$$

where $s_e,\ s_n\ ,\ s_c,\ and\ s_a$ are the slopes in the east, north, along-track, and cross-track directions, respectively. The grids of longitudes (e) and latitudes (n) are equally spaced at 2 km intervals in the cross-track (c) and along-track (a) directions. We take the gradient of each of the longitude and latitude grids to construct unit vectors to project the model east and north slopes into cross-track and along-track slopes as follows:

$$\begin{bmatrix} s_c \\ s_a \end{bmatrix} = \begin{bmatrix} \frac{\partial e}{\partial c} & \frac{\partial n}{\partial c} \\ \frac{\partial e}{\partial a} & \frac{\partial n}{\partial a} \end{bmatrix} \begin{bmatrix} s_e \\ s_n \end{bmatrix} \tag{2}$$

where, for example, $\frac{\partial e}{\partial c}$ is the derivative of the east in (i.e., meters longitude scaled by the cosine of the latitude) with respect to the cross-track distance (in meters).

The analytical inverse of this 2x2 projection matrix is used to convert the SWOT along- and cross-track slopes into north and east slopes and ultimately gravity anomaly and vertical gravity gradient. An example of the along-track and cross-track slopes in microradians for ascending pass 011 and descending pass 026 (cycle 541 with a typical SWH of 4.0 m) is shown in Figure 3a,b (no data editing nor crossover correction applied). The gravitational signatures of the Foundations seamounts are clearly visible in single passes of SWOT data and provide the short-wavelength signal for this study.

Using equation 2, we project the east and north model slopes shown, in Figure S4, into the along-track and cross-track directions and subtract them from the SWOT slopes to reveal the residual slopes (Figure 3c,d). There are several features in these residual slopes worth noting. First the residual slopes have a pervasive short-wavelength noise with amplitude of 2-3 μrad. The noise has higher amplitude along the edges of the swaths that we will edit using the quality flag. In addition, the residual cross-track slope from pass 011 is predominantly negative (blue) with an offset of around -2.5 μrad while the cross-track slope from pass 026 has a slight positive bias. This reflects interferometer

baseline roll error to be removed by the height crossover analysis. The quadratic term in roll error will bring a slope to the along-/cross-track slope measurement, disrupting real geoid signals thus not considered in this study. SWOT post-launch evaluation confirms that the error before calibration is primarily at the larger time scales [Ubelmann et al, in prep]. This aligns with the small along-track slope bias, and the larger cross-track slope bias observed in our study. Note the SWOT data and the model are completely independent. Moreover we have not adjusted the SWOT data or model in any way so our analysis reflects the inherent accuracy of the L2_LR_SSH product.

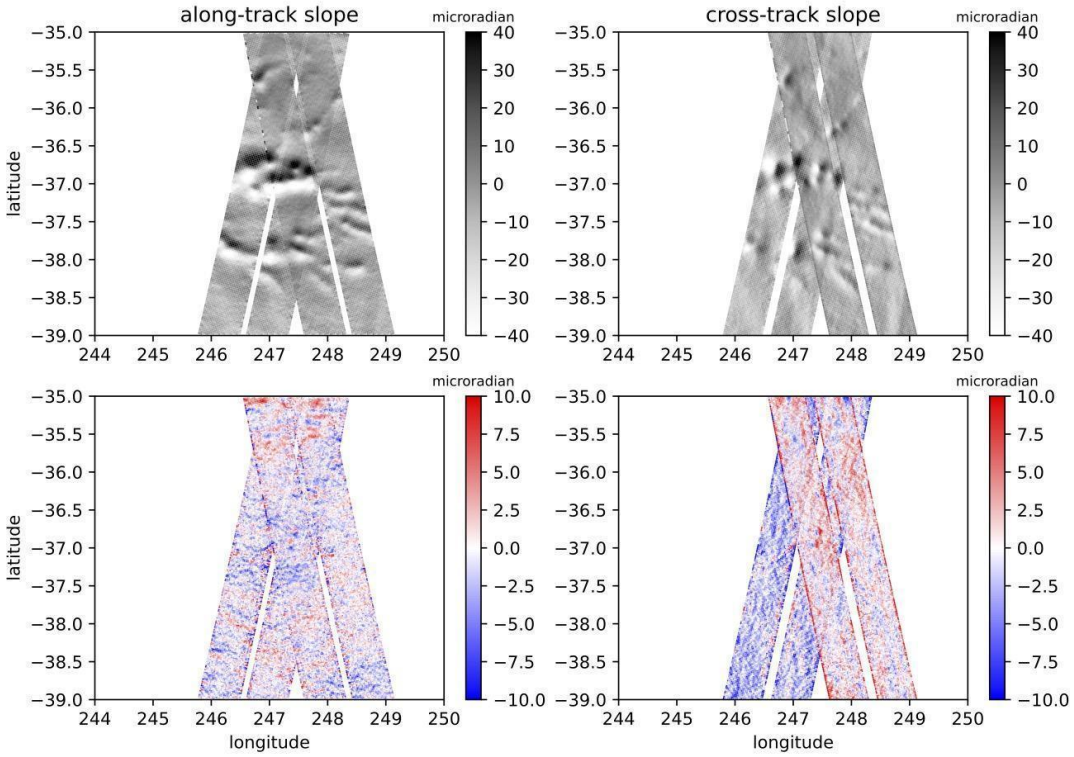

Figure 3. (a) Along-track and (b) Cross-track slope without crossover correction nor data edits for one SWOT cycle (541) along ascending (pass 011) and descending (pass 026). (c) Difference between SWOT along-track slope and model slope shows mainly small spatial scale noise with higher noise on the edges of the swaths. (d) Difference between SWOT cross-track slope and model slope shows noise but also a mean slope difference of -2.5 μrad (Pass 011) due to uncorrected spacecraft roll error.

Accuracy

We now have the components to assess the accuracy and resolution of individual passes of SWOT data as well as stacks of data. The analysis is performed on passes 011 and 026. We report the pass 011 result in the paper and pass 026 result in the supplement.

The accuracy of the SWOT data is established through point-wise comparison of along-track and cross-track slopes with the matching model slopes. An example is shown

in Figure 4, for one cycle (541) as well as the stack of 91 cycles. The along-track slope of the single cycle has a mean of -0.11 μrad and a standard deviation of 2.68 μrad while the stack has a smaller mean of -0.01 μrad and standard deviation of 1.16 μrad. These statistics are better than the comparison of the model gravity with the ship gravity (Figure 2), probably because the ship gravity has some outliers related to sharp turns of the vessel that should be edited. The cross-track SWOT data have similar standard deviations for both the single cycle and the stack. However, the mean cross track differences are significantly larger than in the along-track direction, 0.95 μrad for cycle 541 and 0.57 μrad for the stack. This reflects the residual roll error of the SWOT interferometer. The standard deviation of a single cross-track slope and the stack slope are 2.71 μrad and 1.32 μrad, which is similar to the std in the along-track direction. This is a remarkable achievement since 1 μrad of orientation error of the 10 m long baseline of the interferometer corresponds to a height positional error between the antennas of only 10 micrometers!

The complete analysis of all 91 repeats of pass 011 are provided in Table 1 with a summary in Figure 5. First, we discuss the mean along-track and cross-track slope error. A typical along-track mean slope error is only 0.05 μrad for each cycle. This is based on the median of the absolute value of the mean slope difference. In contrast, a typical cross-track mean slope error is much larger, 0.89 μrad. This is much larger than the model slope error so will need to be adjusted when processing SWOT data for almost any application.

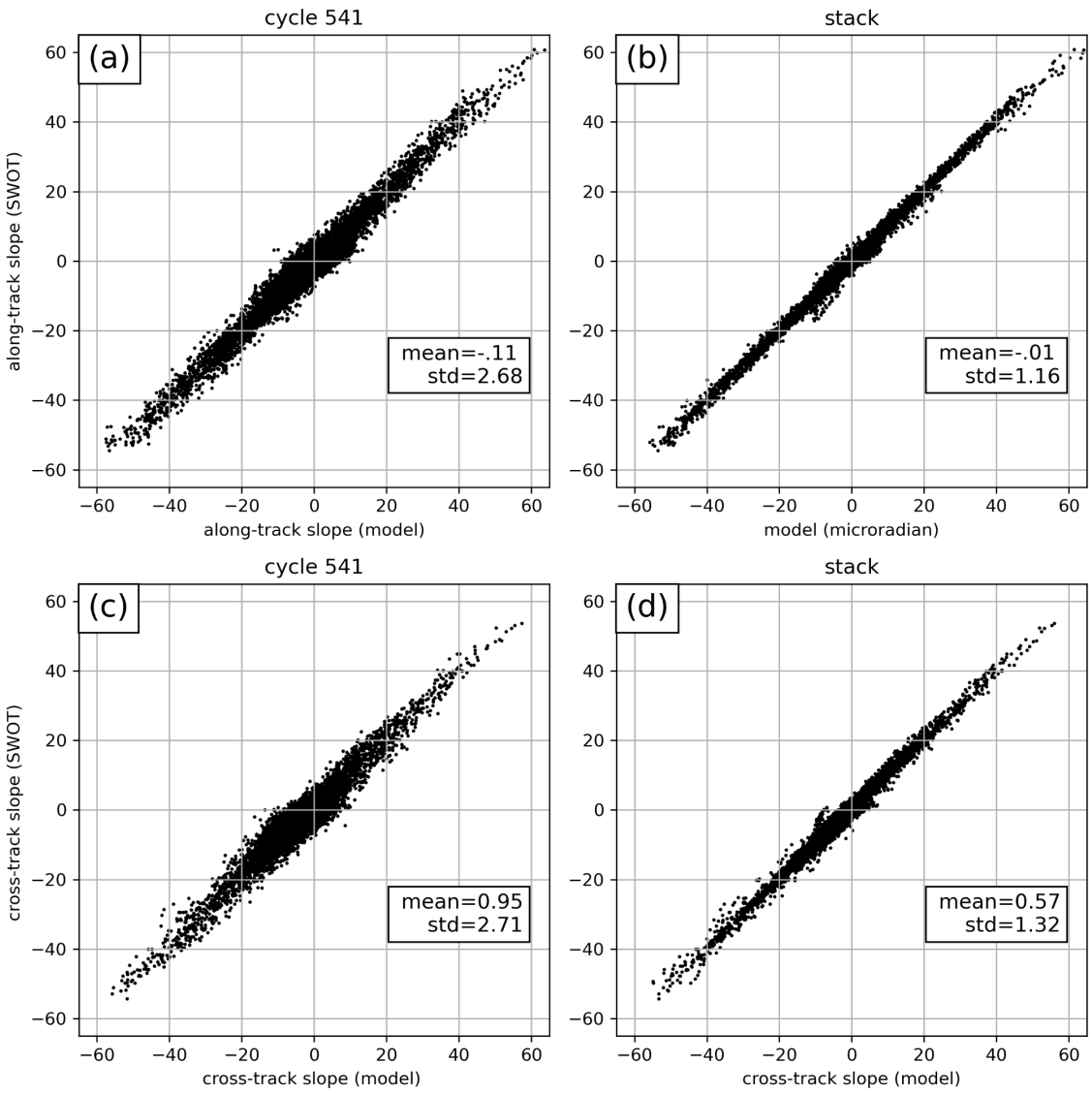

Figure 4. (a) Along-track slope from SWOT (cycle 541) versus model along track slope in the unit of μrad. The mean/standard deviation (std) difference is -0.11 μrad /2.68 μrad. (b) Stacked along-track slope vs model along-track slope. The mean/std difference is -0.01 μrad /1.16 μrad. (c) Cross-track slope from SWOT (cycle 541) versus model along track slope. The mean/std difference is 0.95 μrad /2.71 μrad. (d) Stacked cross-track slope vs model along-track slope. The mean/std difference is 0.57 μrad /1.32 μrad.

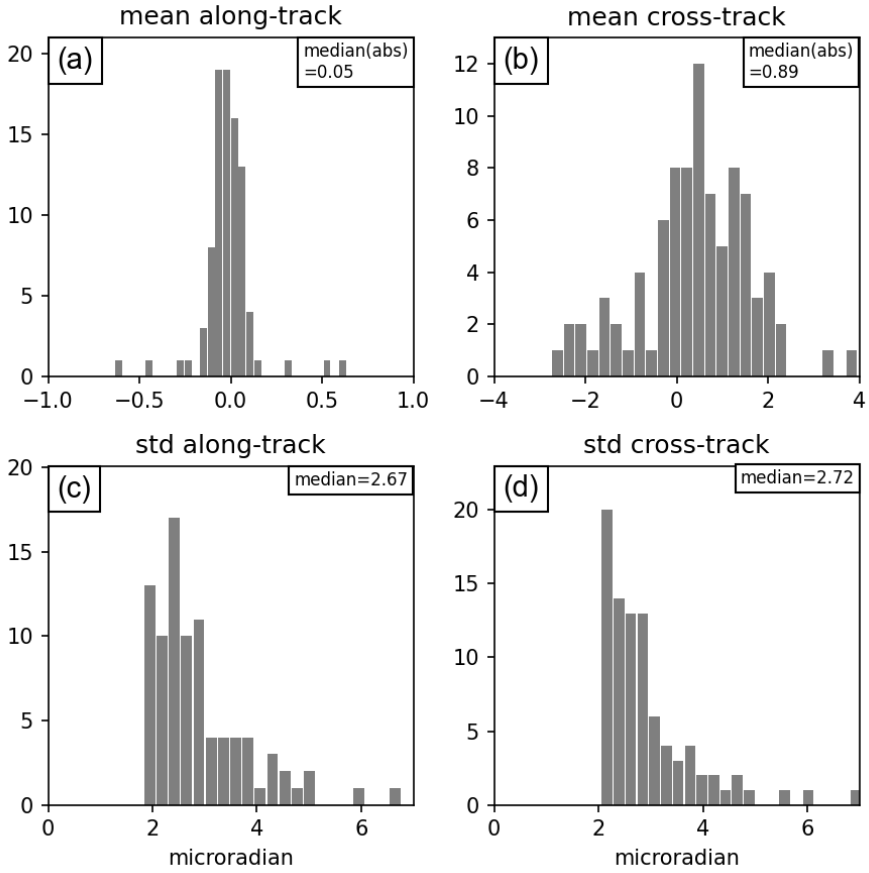

Figure 5. (a) Histogram of the mean difference in along-track slope between the SWOT data and the model (see Table 1). (b) Same histogram for the cross-track slope has typically large absolute deviations of ~0.9 μrad. (c)/(d) Histogram of standard deviation (std) of along/cross-track slope between the SWOT data and the model.

The more interesting result is related to the standard deviation of the along-track and cross-track slope which is typically 2.67 and 2.72 μrad, respectively (see Figure 5 c and d). The L2_LR_SSH data on a 2 km grid are low-pass filtered from the original 250 m grid; the filter has 0.5 gain at a wavelength of 4.5 km [Stiles et al., 2023]. The main source of noise is related to sea surface waves and swell which can have wavelengths up to 500 m in the deep ocean. Because all low-pass filters have side lobes, some of the short (e.g. 500 m) wavelength wave energy can remain after filtering and decimation. To understand this wave-height noise, we compared the standard deviation of the slope difference with the significant wave height (SWH) and distance from the nadir track, both provided with the SWOT L2_LR_SSH data. We divide slope data into 6 groups based on the SWH range and examine the std of slope difference as a function of cross-track distance from the central nadir (Figure 6). As expected, high slope noise is associated with high SWH and the along-track slope (solid lines) has slightly lower noise than the cross-track (dashed lines). When the SWH is less than about 3 m, the slope noise is less than about 2.7 μrad which is the median noise in a single cycle. As the SWH

increases, the noise increases so when the SWH exceeds 6 m, the noise is typically greater than 5 μrad and can be as large as 8 μrad. The slope noise also changes with the cross-track distance. When SWH < 4 m, noise is highest at the outer edge of the swath, showing the effect of roll error. While SWH > 4m, noise is the highest close to the central nadir. This relationship between slope noise and SWH provides a basis for weighting the contributions to the stack by 1/SWH. We performed the same analysis on descending pass 026, as well using the L3 data (both passes) and the results are similar (see Tables S1 and S2).

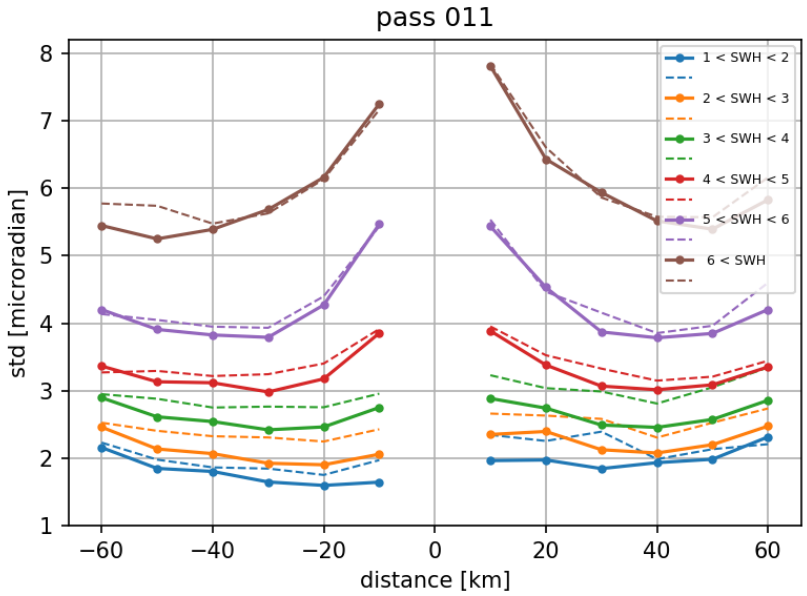

Figure 6. standard deviation (std) difference between 90 cycles of along-track slope and along-track model as a function of SWH and the distance to the Nadir point. Solid lines with dots are std for along-track slope difference while dashed lines for the cross-track slope difference.

Resolution

The analysis of point-wise along-track slope (Table 1 and Figure 4) provide the overall accuracy of the SWOT data. However, there is no information on how the correlation changes with wavelength or at which wavelength the SWH noise dominates the gravity signal. To address these questions, we perform spectral and cross-spectral analysis of the SWOT data and the difference between the SWOT data and the along-track model slope.

We show the power spectral density (PSD) of the SWOT along-track slope and its noise from cycle 541 (Figure 7a) and the stack slope (Figure 7b). The noise is calculated as the difference with the model along-track slope. The stack slope is constructed using 64 high-quality cycles and 1/SWH as weight. There are 27 out of 91 cycles not used because of large data gaps. Data with SWH > 6m are not used.

The spatial resolution of the SWOT L2_LR_SSH data is determined by performing a cross-spectral analysis [Bendat and Piersol, 1986] between the along-track slope from SWOT and the model along-track slope. We examine the coherence with the model

along-track slope using a single cycle (cycle 541) of SWOT slope (Figure 7c), as well as the SWOT stack slope. SWOT data are edited using the quality flag and each complete column (211 points, called “number of lines” in SWOT L2 data files) of the along-track SWOT and model grids are Hann windowed then zero-padded to 512 points. There are 53 columns (called “number of pixels” in the SWOT L2 data files) without data gaps to compute the coherence using the Welch method. We concatenate the 53 columns and use a 512-point segment length and zero overlap to calculate the cross-spectral coherence between SWOT slope and model slope. For a single cycle, the coherence drops to 0.5 at around 14.2 km (Figure 7c) where we can also see agreement in energy between the SWOT slope and SWOT slope noise (Figure 7a). For the stack slope, SWOT shows a spatial resolution of about 8.0 km (Figure 7d), better than the resolution of the current best marine gravity field (~10 km) [ref]. There is higher energy in SWOT stack slope noise than stack slope, indicating errors in the MSS model are higher than SWOT stack slope, thus our estimate of 8.0 km resolution could be conservative.

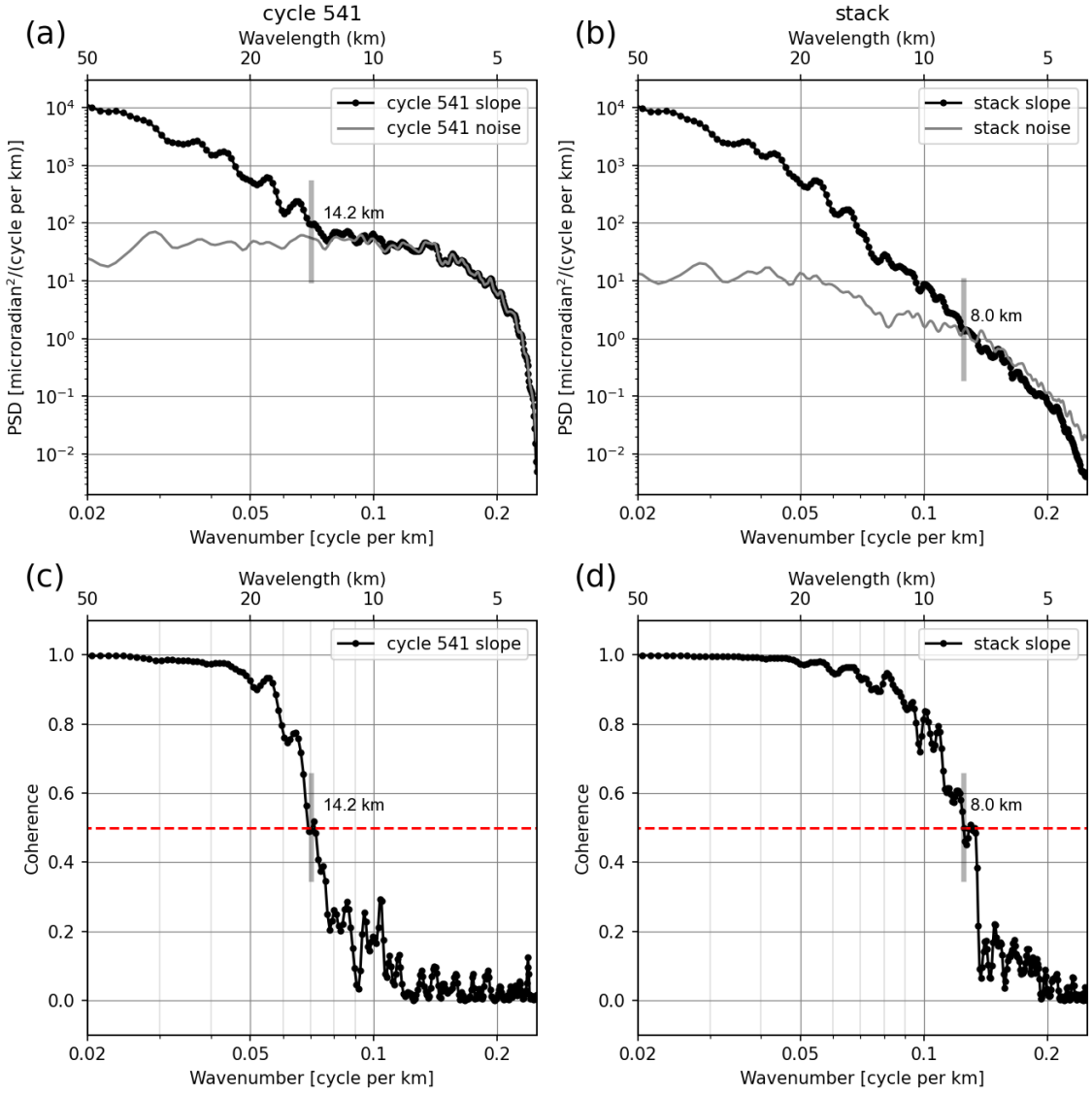

Figure 7. (a) Power spectral density (PSD) of along-track slope for cycle 541 (black curve) and the difference between the SWOT slope and model slope reflects the noise (gray curve). (b) PSD for stack of 53 cycles for pass 541 (black curve) and the difference between SWOT stack slope and model slope (grey curve). The power in the stacked slope noise is about 35 times lower than the individual cycle at a wavelength of 10 km. (c) Cross-spectral coherence between cycle 541 (along-track) and the model falls to 0.5 at a wavelength of 14.2 km. (d) Cross-spectral coherence between stack (along-track) and the model falls to 0.5 at a wavelength of 8.0 km.

Discussion

The swath altimeter aboard SWOT is a radar interferometer that measures height differences along and across the swath. Like any interferometer, the phase, or height, has a $2N\pi$ ambiguity that can be resolved using the nadir altimeter or a general knowledge of the mean sea surface height or geoid height. For our applications in marine gravity and bathymetry, knowledge of absolute height is unnecessary; we utilize the derivatives of the geoid including first derivatives such as geoid gradient (i.e., deflections of the vertical (VD)) and gravity anomaly, as well as second derivatives such as vertical gravity gradient. Standard nadir altimetry can be used to estimate the MSS height however because each profile has long-wavelength errors associated with orbit, atmospheric corrections, tides and other oceanographic effects one must generally performs a crossover correction prior to the construction of the MSS [Andersen and Knudsen, 2020; Schaeffer et al., 2023]. When the multiple altimeter profiles are gridded, the small cross-track residual height error introduces small-scale noise in the MSS. This noise is significantly reduced by taking the along-track derivative of each profile prior to gridding [Olgiati et al., 1995; Sandwell and Smith, 1997; Yu et al., 2021]. Moreover, the derivative operations transform the normally red spectrum of MSS/geoid to something closer to a white spectrum. A significant benefit of this pre-whitening is it reduces edge effects in any kind of spectral analysis. The downside of taking derivatives of nadir altimeter data is that the short wavelength white noise is transformed to a “blue” noise so a carefully-designed low-pass filter is needed to suppress the noise.

The best marine gravity anomaly models from nadir altimeters have accuracy of 2-3 mGal and must be low-pass filtered at a wavelength of at least 14 km to suppress the short wavelength noise that has been amplified by taking derivatives. As we demonstrate in this study, this accuracy and resolution is insufficient to assess the quality of the SWOT data so we have used the very high resolution seafloor bathymetry in the Foundation seamounts area to improve the accuracy to 1.42 mGal and a resolution of 6.8 km based on a comparison with very high quality shipboard gravity. Nevertheless, we do not know whether the tuned-up altimeter-derived gravity is more or less accurate than the ship gravity.

Our analysis of individual cycles of SWOT data shows a standard deviation that is typically 2.6 μrad and a resolution of 14.2 km which is approaching the quality of the

marine gravity based on 20 years of nadir altimetry [Sandwell et al., 2021]. The standard deviation increases with increasing SWH (Figure 6). The single-cycle SWOT noise has a relatively flat spectrum between wavelengths of 50 and 5 km where the low-pass filter dominates (Figure 7a). This flat noise spectrum is unlike standard nadir altimetry where the height spectrum is white and the slope spectrum is blue. Therefore, any additional filtering needed to reduce noise should be applied to the SWOT slopes rather than the heights.

Stacking 60+ repeats of SWOT improves the standard deviation to ~1.2 μrad and the resolution to ~8 km. After stacking, both the signal and noise have a red spectrum with a slope of ~k^{-6} (Figure 7b). Note this analysis is based on the comparison of the model vertical deflection grids which are not perfect. Indeed, after stacking, the noise at wavelengths less than 8 km (grey curve) is higher than the SWOT signal (black curve) . Since the noise is the difference between the model slope and the SWOT slope, the model noise must be larger than the SWOT noise, suggesting our estimates for the accuracy and resolution of the stacked SWOT slopes are conservative.

All of these comparisons are performed without performing any kinds of data adjustments. However, we find that the mean cross-track slope typically differs from model slope by 0.9 μrad and sometimes this mean slope error exceeds 4 μrad for an individual cycle of pass 011. We suggest that the mean cross-track slope difference should be removed prior to construction of improved gravity products [Yu et al., 2021]. In contrast, the along-track slope mean slope differences are generally much smaller (~0.05 rad) than the noise in the stacked slope (~1.2 μrad).

Pass 026 of SWOT L2 data shows similar or slightly better performance compared to pass 011. Pass 026 has a standard deviation that is typically 2.6 μrad and a resolution of 13.0 km. The differences with the model slope in the cross-track direction is similar to in the along-track direction (Table S2).

The L3 data are on the same 2 km by 2 km grids as L2 data [Dibarboure et al., in prep] and they are calibrated to be in consistency with radar altimeters. The performance of L3 datasets are very similar to L2 over the Foundation Seamounts: 1) for a single cycle, it shows a similar precision of about 2.6 μrad and spatial resolution of about 13.0 km; 2) for the stack of ~90 cycles, it shows 1.2 μrad in standard deviation and 8 km in spatial resolution. L3 datasets are expected to be a significant improvement upon L2 calibration for 1-day orbit regions far away from 1-day crossovers (e.g. near the equator). The Foundation seamounts being exactly on a crossover explains the little difference between L2 and L3 products. When compared with model slopes, we find a slightly larger typical offset in the cross-track direction (~0.12 μrad) than in the along-track direction (0.03 μrad) (Table S3), suggesting that further efforts on crossover error removal are needed.

One scenario for improving the global marine gravity using 2 km resolution SWOT data is to: 1) Remove along-track and cross-track model slopes from the SWOT data using the best available vertical deflection grids based on nadir altimetry. 2) Remove the mean cross-track slope difference over segments of perhaps 2000 km. Our analysis does not provide information on how the cross-track slope error varies along the track. 3) Stack the along- and cross-track slopes using a weighting based on the ~1/SWH. 4) Project the along- and across-track stacked residual slopes into the east and north directions using the inverse of equation (2). 5) Perform a block median of residual east and north slopes and grid them using a spline in tension algorithm such as the GMT *surface* program. There will be diamond-shaped areas having no SWOT coverage so areas further than about 4 km from a SWOT measurement should be padded to zero prior to gridding to suppress spline overshoots. 6) Finally add the model slopes to the gridded residual slopes. At this point one could compute gravity anomaly or any higher derivatives of the gravity field.

Our SWOT data evaluation is performed over the Foundation Seamounts where ocean noise is one or two orders of magnitude smaller than geoid signals. Nevertheless, our conclusions can also be applied in regions where ocean signals cannot be ignored. SSHA is a zero-centered random process with temporal correlation, it will average to zero almost like noise using many repeats [Dibarboure and Pujol, 2021].

This entire analysis mainly pertains to the construction of marine gravity products from SWOT although aspects of the processing and analysis are also relevant for extracting small-scale oceanographic signals from SWOT data. One important issue related to marine gravity is that, because of the natural upward continuation low-pass filter, the amplitude of the gravity signal at wavelengths less than the mean ocean depth is vanishingly small. Consider, for example, a 10 mGal amplitude gravity anomaly having a wavelength of 8 km measured just above the seafloor having a depth of 4000 m. Because of Newton's law, the amplitude of this anomaly measured on the sea surface will be attenuated by $exp\left(-\frac{2\pi z}{\lambda}\right) = 0.043$. The attenuation of this natural low-pass filter is stronger than the low-pass filter used to construct the 2 km resolution SWOT ocean product from the 250 m SWOT data [Stiles et al., 2023]. Therefore, except in rare cases of shallow ocean (< 400 m in depth) and large amplitude gravity, the 2-km grid supplied with the L2_LR product will be nearly optimal for constructing marine gravity products. In coastal regions, the 250-m grid product is needed and errors related to barotropic tides and internal internal tides need to be considered carefully.

Another important result of the natural upward continuation filter is that one can be confident that anomalies having wavelengths less than about 8 km are not caused by residual error in the MSS or SSS models; these anomalies must be true oceanographic signals or noise. There are several benefits when working with gradients rather than heights. First, as discussed above, the short-wavelength (< 30 km) noise in the model gradient grids is smaller than the short wavelength noise in the model MSS grids so one

can isolate smaller oceanographic signals using slopes rather than heights. In addition, since the slope noise is relatively white having amplitude of ~2.5 μrad, one can easily estimate the observation threshold amplitude of a shorter wavelength wavelike signal, for example an ocean surface wave with 40 mm amplitude and 4 km wavelength will exceed the slope noise in the 250 m ocean product.

A final question related to the science part of the SWOT mission is how many repeat cycles will be needed to make a significant improvement in the global marine gravity derived from all nadir altimeters? For pass 011, the standard deviation between the original VD grids (V32) and the improved model grid using shipborne data is 1.50 μrad for the east component and 1.44 μrad for the north component. We show that by stacking 60+ repeats, an accuracy of 1.2 μrad and a spatial resolution of 8 km can be achieved (Figures 4b and 8c). For each specific number of cycles used, we bootstrap the 60+ repeats with 50 realizations to obtain the along-/cross-track standard deviation, and the associated 95% confidence interval, between the SWOT stack and the model stack versus the number in the stack, as depicted in Figure 8a. The cross-track standard deviation is somewhat higher than the along-track because of the higher noise on the edges of the swaths as seen in Figure 1d, although some of the edge noise was removed using the quality flag. If we just consider the stacked along-track slopes it will take 8 repeat cycles for the accuracy of the SWOT along-track slope to match the accuracy of the north component of the V32 VD. In terms of resolution, we constructed the spatial resolution versus the number of cycles used (Figure 8b) using similar methods as for the standard deviation. It will take 11 cycles for the SWOT VD to match the 10-km resolution of the V32 VD. After about 20 repeat cycles, the SWOT gravity field will be significantly better than the current gravity models based on nadir altimetry. Note it has taken 232 months of nadir geodetic mission data to achieve the accuracy of the current models so a significant improvement in just 14 months is a major achievement. Of course this is a conservative estimate because some fraction of the standard deviation between the stacked SWOT slopes and the model slopes is due to remaining error in the model and the magnitude of this error is largely unknown.

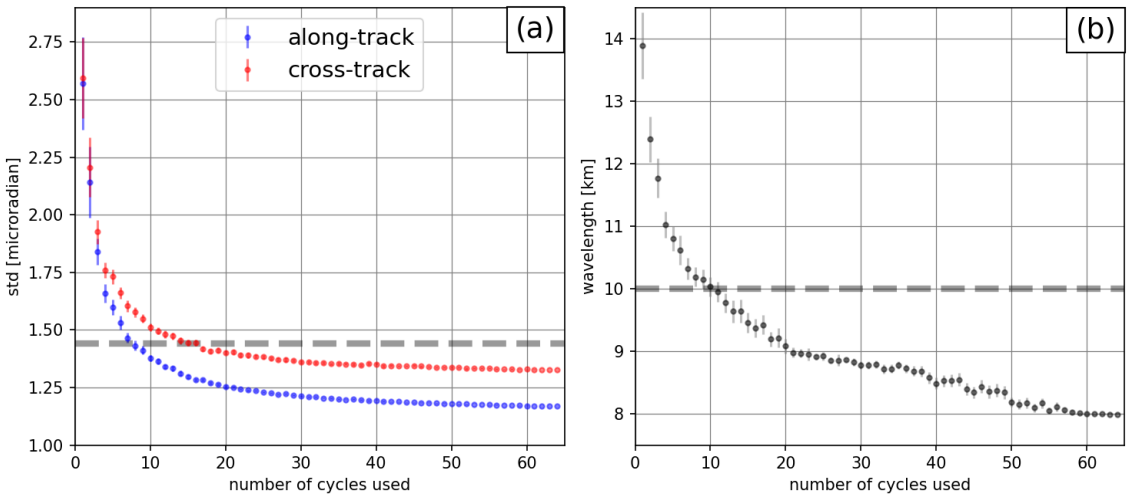

Figure 8 (a) Standard deviation of the difference between along-/cross-track SWOT stacked slopes and the model slope versus the number of cycles used in the stack. (b) Spatial resolution of along-track slope (coherence 0.5) versus number of cycles in the stack. The end members for 1 cycle and 64 cycles are shown in Figures 4 and 7. Grey dashed lines are the current accuracy (a) and resolution (b) of the V32 altimeter-only model. Error bars show the 95% confidence interval. Improvements from SWOT will require ~11 repeat cycles in the 21-day science orbit.

Conclusions

- The Foundation seamounts area provides a unique opportunity to assess the accuracy and resolution of the marine gravity field that will be recovered by SWOT. The area has complete multibeam coverage and highly-accurate shipboard gravity profiles to construct east and north grids of deflection of the vertical for comparison with along-/cross-track sea surface gradients measured by SWOT.
- A single cycle of SWOT coverage, at a typical SWH of 2-3 m, has a precision of 2.6 μrad and a spatial resolution of 13 km. The mean along-track slope is commonly within 0.05 μrad of the model slope while the mean cross track slope error is somewhat larger ~0.9μrad - 2.0 μrad. The mean cross-track slope from SWOT should be adjusted to the model slope before constructing marine gravity.
- The slope noise increases significantly for SWH above 5 m so cycles should be weighted by ~1/SWH during stacking.
- A stack of ~60 cycles of SWOT data provides a dramatic improvement in precision ~1.2 μrad and spatial resolution ~8 km. This dramatic increase in accuracy and, especially resolution, would reveal much more detail in small-scale seafloor structures such as seamounts and abyssal hills.
- The accuracy and resolution of the marine gravity field derived from SWOT will exceed the accuracy of the current models after 11 repeat cycles (~8 mo.). Significant increases will require about 20 repeat cycles (~14 mo.).
- The optimal method for improving the gravity field from SWOT data will use sea surface gradients projected into the north and east directions and combined with existing models using a standard remove-grid-restore method.

Acknowledgements

This work was supported by the NASA SWOT program (80NSSC20K1138), the Eric and Wendy Schmidt AI in Science Postdoctoral Fellowship, a Schmidt Futures program and the Office of Naval Research (N00014-17-1-2866). The Generic Mapping Tools (GMT) (Wessel et al., 2019) were extensively used in data processing. We appreciate the efforts from everyone who works for the SWOT mission.

Supplementary Material

This supplementary material provides the details on how the altimeter-derived gravitational field is enhanced using high resolution multibeam bathymetry as calibrated

using shipboard gravity. Note that by using a published gravitational model such as EGM2008 [Pavlis et al., 2012] one can easily calculate the various components of gravity since they are all related by Laplace's equation. These include geoid height, deflections of the vertical, gravity anomaly, and all the components of the gravity gradient tensor. At wavelengths > 100 km, the spherical harmonic coefficients enable computation of any of these quantities. At wavelengths < 100 km, Fourier series, in a Cartesian coordinate system, provide the most accurate and efficient method of computation of any of these quantities. Here we will focus on using the along-track slope of standard radar altimeter profiles to compute the north and east components of the deflection of the vertical [e.g., Sandwell and Smith, 1997].

We begin with the most recent version of the gravity field (V32) derived at SIO using all the standard altimeter profiles data that were available in August of 2022. Near global grids spanning latitude of +/- 81.7 degrees are available as: mean sea surface, east and north deflections of the vertical, free-air gravity anomaly/uncertainty and vertical gravity gradient (https://topex.ucsd.edu/pub/global_grav_1min/). We note that the MSS has a lower accuracy and spatial resolution at short wavelengths than the other derivative components. The deflections of the vertical and gravity anomaly have the best accuracy and resolution because they are derived directly from along-track altimeter slope measurements. The along-track derivative operation suppresses any long wavelength errors due to ocean tides, ocean dynamics, atmospheric loading, and sea state bias. Differentiation also amplifies altimeter noise, mostly due to ocean waves so we have re-tracked all the original altimeter waveforms using an algorithm that reduces this SWH noise by about a factor of 1.5. Moreover, the along-track slope data are low-pass filtered and carefully edited in a consistent way [Yu et al., 2022]. To begin the enhancement process, the EGM 2008 model [Pavlis et al., 2012] is removed from the altimeter height profiles so gridding, filtering, and conversion to other products is done in the Cartesian space using a fast Fourier transform algorithm.

All the along-track slope data and associated uncertainties are gridded into east and north slopes using radial basis functions based on biharmonic splines in tension [Wessel and Bercovici, 1998]; there is no intermediate MSS or geoid product. Finally, the north and east grid are low-pass filtered in the Fourier transform domain using a cosine function with a 0.5 gain that is a function of mean ocean depth (14 km for depth < 3.5 km, 15 km for depths between 3.5 and 4.5 km, 16 km for depth between 4.5 and 5.5 km, and 17 km for deeper depth). In addition, the vertical deflection grids are converted to gravity anomaly and the long-wavelength EGM 2008 product, that was removed from the original altimeter heights, is restored.

At this point, the relevant products are the east and north deflections of the vertical, and the matching free-air gravity anomaly. Note that all the products are low-pass filtered at a wavelength of 14 km or longer. However, to assess the accuracy and resolution of the SWOT data we need vertical deflection grids that are at least as accurate as the SWOT data and retain wavelengths as short as the low-pass filter of 4.5 km that is applied to 2 km by 2 km the L2_LR_SSH product.

The accuracy and resolution of the altimeter-only, vertical deflection grids are improved using a gravitational model generated from the high resolution multibeam bathymetry in the region (Figure 1). The gravity field for flexurally compensated topography depends primarily on the two density interfaces – the seafloor topography and the Moho topography. The main assumptions are that the density of the seafloor topography is uniform and the oceanic lithosphere responds linearly as a thin elastic plate isostatically floating on the higher density mantle. The important parameters are the density of the seafloor and the thickness of the elastic plate. For a more complete discussion see the book by Watts [2001] as well as the excellent paper by Parker [1973]. All of this theory, including the exact, non-linear gravitational model for the uneven topography, is implemented in Generic Mapping Tools (GMT) in a routine called *gravfft.* The topography used for the analysis is a 1 minute gridded topography that combines the multibeam mapping of the Foundation seamounts with gravity predicted depth and any other bathymetry in the region [Tozer et al., 2019] (Figure 1). The selected region (-124/-104/-42/-30) is larger than the region used for the misfit evaluation to reduce model edge effects.

The algorithm for determining the best fit density and elastic thickness involves the following:

1. Loop over a plausible range of elastic thickness and crustal density.
2. Compute the isostatic gravity anomaly using *gravfft.*
3. High-pass filter the model gravity using a Gaussian filter with a 0.5 gain at 40 km wavelength.
4. Low-pass filter the altimeter-derived gravity model using the same Gaussian filter.
5. Add the two models and compute the rms difference between the combined model and the much higher accuracy ship gravity data (white line in Figure 1 and blue curve in Figure S1).

We found the lowest rms misfit is a model having a density of 2600 kg m^{-3} and elastic thickness T_e of 4 km (Table S1). The components and final results are shown in Figure S2. The original altimeter-only gravity (Figure S2a) is combined with the topography-only gravity (Figure S2b) using a crossover wavelength of 40 km (Figure S2c). The difference between the combined model and the altimeter only (Figure S2d) shows many short wavelength peaks in the gravity associated with shallow seamount summits that were not resolved in the altimeter-only model.

Figure 2a shows a plot of model gravity versus ship gravity having a standard deviation of 1.96 mGal (1.42 mGal median absolute deviation). Note that 1 μrad of slope error corresponds to 0.98 mGal of gravity error. Figure 2b shows the spectral coherence between the model gravity and the ship gravity. The 0.5 coherence occurs at a wavelength of 6.8 km. The altimeter-only has a 0.5 coherence at 10 km which is inadequate for assessment of the higher resolution SWOT data.

The final step is to construct models of east and north vertical deflection (i.e., the negative of the sea surface gradient). This is accomplished by computing the east and north vertical deflection using the *gravfft* routine with the optimal parameters and combining with the altimeter-only vertical deflections using the 40 km crossover wavelength. Based on this analysis, we expect the accuracy of the model vertical deflection grids to be 1.98 μrad and the spatial resolution to be 6.8 km. We now have the components to assess the accuracy and resolution of the SWOT data.

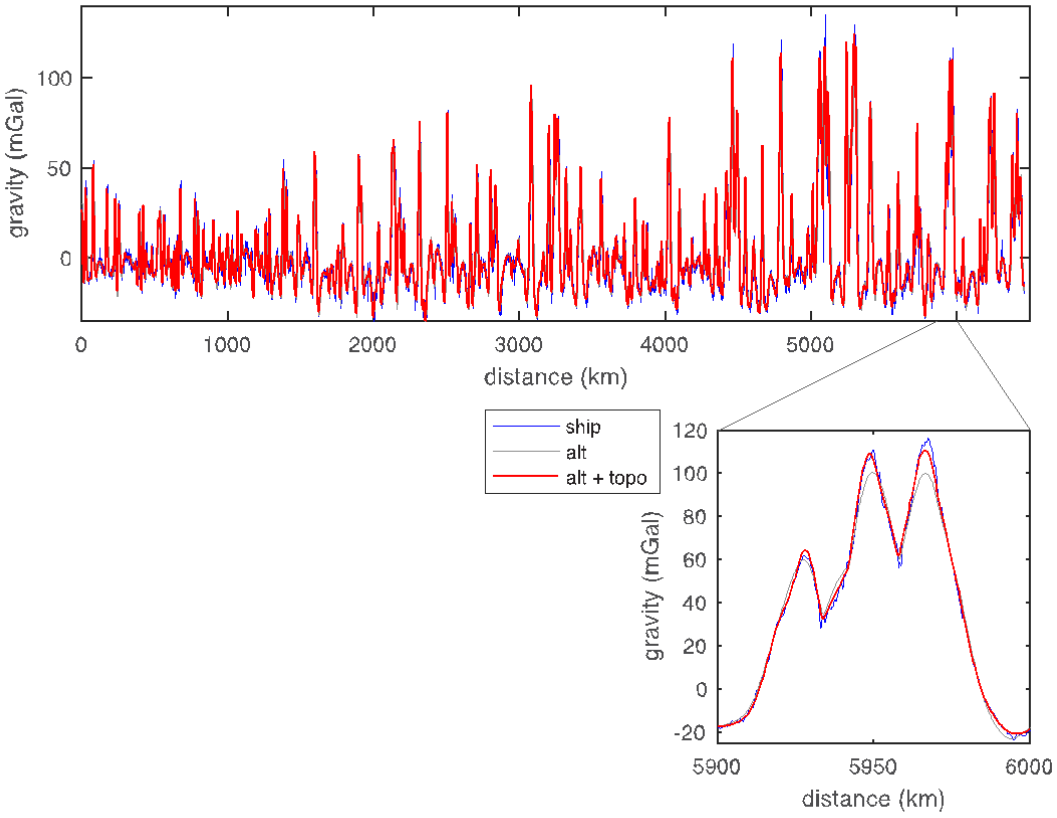

Figure S1. Gravity versus distance along the L' Atalante trackline shown in Figure 1, ship gravity (blue), altimeter gravity (grey), and combined altimeter/topography gravity (red). The median absolute deviation (mad) between the altimeter and ship gravity is 2.05 mGal and between the combined and ship gravity is 1.42 mGal (1 mGal ~ 0.98 microradian).

Table S1. Estimating seafloor density and elastic thickness

Density (kg m^{-3})	Mean (mGal)	Std (mGal)	Median (mGal)	Mad (mGal)	Slope (a-t/ship)	Slope (ship/a-t)	Te (km)
alt-only	0.014	2.88	0.071	2.05	0.964	1.022	-
2400	-0.051	2.31	0.089	1.65	0.952	1.043	4
2500	0.081	2.04	0.117	1.48	0.976	1.017	4
2550	0.149	1.97	0.131	1.43	0.990	1.003	4
2600	**0.215**	**1.96**	**0.137**	**1.42**	**1.002**	**0.992**	**4**
2650	0.284	2.02	0.144	1.45	1.016	0.978	4
2700	0.351	2.14	0.159	1.51	1.028	0.967	4
2800	0.488	2.50	0.155	1.73	1.054	0.943	4
2600	0.071	1.97	0.078	1.43	0.977	1.017	2
2600	0.266	2.01	0.142	1.45	1.010	0.983	6

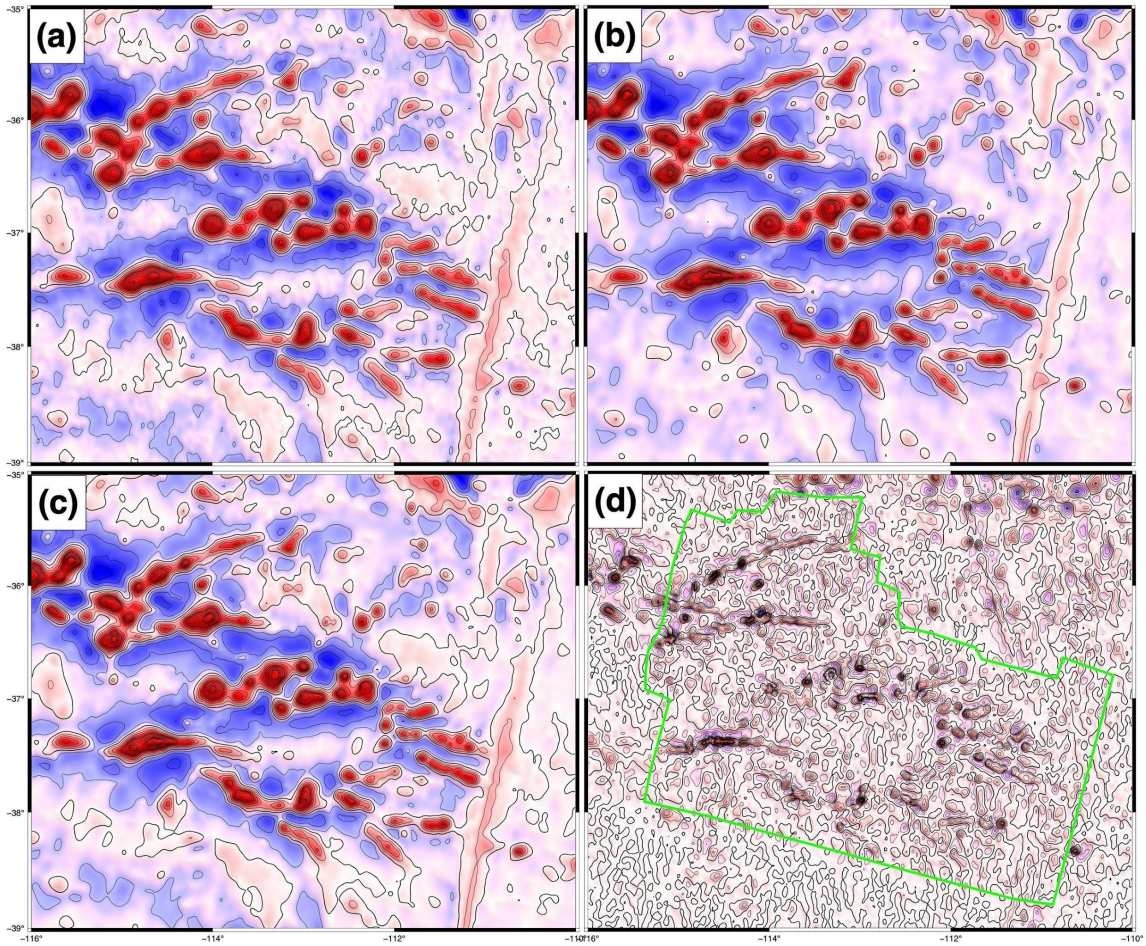

Figure S2. (a) Gravity anomaly from satellite altimetry (10 mGal contours). (b) Gravity anomaly from seafloor topography (density 2600 kg m^{-3}). (c) Combined altimetry/topography gravity using

a crossover wavelength of 40 km. (d) Difference between combined gravity and altimeter gravity (2 mGal contours).

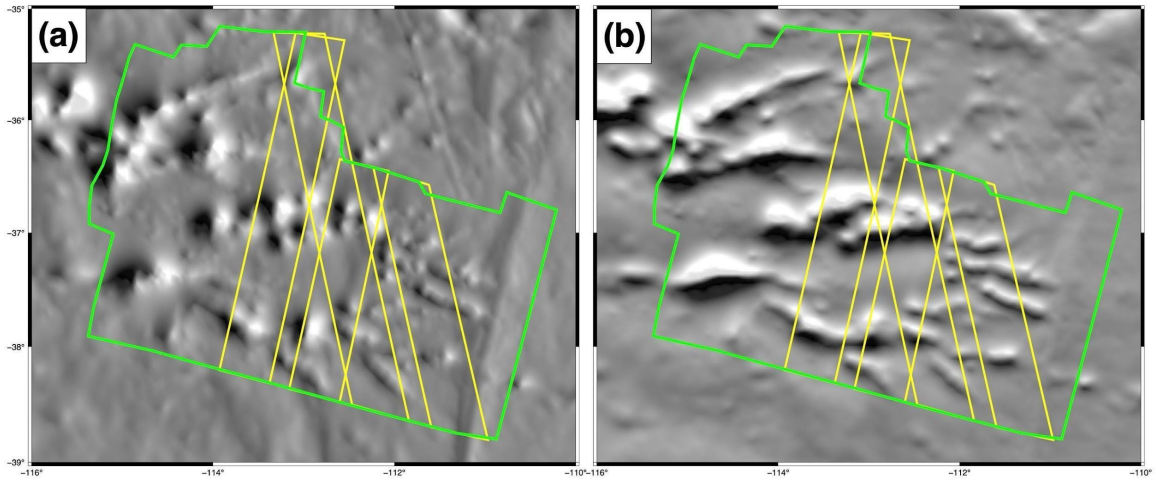

Figure S3. (a) East component of sea surface slope based on combined slopes from altimetry and multibeam topography (gray scale +/- 40 μrad). (b) North component. Green line shows perimeter of multibeam coverage. Yellow polygons mark the swaths of the SWOT altimeter.

References

Andersen, O. B., & Knudsen, P. (2020). The DTU17 global marine gravity field: First validation results. In *Fiducial Reference Measurements for Altimetry: Proceedings of the International Review Workshop on Satellite Altimetry Cal/Val Activities and Applications* (pp. 83-87). Springer International Publishing.

Bendat, J. G. and A. G. Piersol, (1986) Random Data Analysis and Measurement Procedures, 2nd ed. New York: Wiley.

Dibarboure, G., & Pujol, M. I., (2021). Improving the quality of Sentinel-3A data with a hybrid mean sea surface model, and implications for Sentinel-3B and SWOT. *Advances in Space Research*, *68*(2), 1116-1139.

Dibarboure, G., Ubelmann, C., Flamant, B., Briol, F., Peral, E., Bracher, G., Vergara, O., Faugère, Y., Soulat, F. and Picot, N., (2022). Data-Driven Calibration Algorithm and Pre-Launch Performance Simulations for the SWOT Mission. *Remote Sensing*, *14*(23), p.6070.

Devey, C.W., Hékinian, R., Ackermand, D., Binard, N., Francke, B., Hémond, C., Kapsimalis, V., Lorenc, S., Maia, M., Möller, H. and Perrot, K., (1997). The Foundation Seamount Chain: a first survey and sampling. Marine geology, 137(3-4), pp.191-200.

Fu, L.L., Alsdorf, D., Rodriguez, E., Morrow, R., Mognard, N., Lambin, J., Vaze, P. and Lafon, T.,(2009) The SWOT (Surface Water and Ocean Topography) mission: Spaceborne radar interferometry for oceanographic and hydrological applications. *Proceedings of OCEANOBS*, *9*, pp.21-25.

JPL Internal Document, 2018 : Surface Water and Ocean Topography Mission (SWOT) Project Science Requirements Document, JPL D-61923, Rev. B

Maia, M., & Arkani-Hamed, J. (2002). The support mechanism of the young Foundation Seamounts inferred from bathymetry and gravity. Geophysical Journal International, 149(1), 190-210.

Mammerickx, J. (1992). The Foundation Seamounts: tectonic setting of a newly discovered seamount chain in the South Pacific. Earth and planetary science letters, 113(3), 293-306.

Morrow, R., Fu, L. L., Ardhuin, F., Benkiran, M., Chapron, B., Cosme, E., ... & Zaron, E. D. (2019). Global observations of fine-scale ocean surface topography with the surface water and ocean topography (SWOT) mission. *Frontiers in Marine Science*, *6*, 232.

Olgiati, A., Balmino, G., Sarrailh, M., & Green, C. M. (1995). Gravity anomalies from satellite altimetry: comparison between computation via geoid heights and via deflections of the vertical. *Bulletin géodésique*, *69*, 252-260.

Parker, R. L. (1973). The rapid calculation of potential anomalies. Geophysical Journal International, 31(4), 447-455.

Pavlis, N. K., Holmes, S. A., Kenyon, S. C., & Factor, J. K. (2012). The development and evaluation of the Earth Gravitational Model 2008 (EGM2008). Journal of geophysical research: solid earth, 117(B4).

Sandwell, D. T., & Smith, W. H. (1997). Marine gravity anomaly from Geosat and ERS 1 satellite altimetry. Journal of Geophysical Research: Solid Earth, 102(B5), 10039-10054.

Sandwell, D. T., Harper, H., Tozer, B., & Smith, W. H. (2021). Gravity field recovery from geodetic altimeter missions. *Advances in Space Research*, *68*(2), 1059-1072.Sandwell, D. T., Harper, H., Tozer, B., & Smith, W. H. (2021). Gravity field recovery from geodetic altimeter missions. Advances in Space Research, 68(2), 1059-1072.

Schaeffer, P., Pujol, M. I., Veillard, P., Faugere, Y., Dagneaux, Q., Dibarboure, G., & Picot, N. (2023). The CNES CLS 2022 Mean Sea Surface: Short Wavelength

Improvements from CryoSat-2 and SARAL/AltiKa High-Sampled Altimeter Data. *Remote Sensing*, *15*(11), 2910.

Stiles, B., P. Dubois, C.Chen, A. Bohe, L. Fu, R. Morrow (2023). Surface Water and Ocean Topography Project Algorithm Theoretical Basis Document Long Name: Level 2 KaRIn Low Rate Sea Surface Height Science Algorithm, Short Name: L2_LR_SSH, California Institute of Technology, NASA Jet Propulsion Lab, 88 pp.

Tozer, B., Sandwell, D. T., Smith, W. H., Olson, C., Beale, J. R., & Wessel, P. (2019). Global bathymetry and topography at 15 arc sec: SRTM15+. Earth and Space Science, 6(10), 1847-1864.

Watts, A. B. (2001). Isostasy and Flexure of the Lithosphere. Cambridge University Press.

Wessel, P., & Bercovici, D. (1998). Interpolation with splines in tension: a Green's function approach. Mathematical Geology, 30, 77-93.

Wessel, P., Luis, J. F., Uieda, L., Scharroo, R., Wobbe, F., Smith, W. H., & Tian, D. (2019). The generic mapping tools version 6. Geochemistry, Geophysics, Geosystems, 20(11), 5556-556.

Yu, D., Hwang, C., Andersen, O. B., Chang, E. T., & Gaultier, L. (2021). Gravity recovery from SWOT altimetry using geoid height and geoid gradient. *Remote Sensing of Environment*, *265*, 112650.

Yu, Y., Sandwell, D. T., & Gille, S. T. (2023). Seasonality of the Sub-Mesoscale to Mesoscale Sea Surface Variability From Multi-Year Satellite Altimetry. *Journal of Geophysical Research: Oceans*, *128*(2), e2022JC019486.